J Mater Sci (2010) 45:4805–4812
DOI 10.1007/s10853-010-4635-9

ULTRAFINE GRAINED MATERIALS

The ductile to brittle transition of ultrafine-grained Armco iron: an experimental study

A. Hohenwarter · C. Kammerhofer · R. Pippan

Received: 11 February 2010 / Accepted: 18 May 2010 / Published online: 4 June 2010

Abstract Fracture toughness measurements on bcc iron (Armco-iron), which is subjected to severe plastic deformation (SPD), were performed. Through high pressure torsion, an ultrafine grain structure was obtained and with subsequent heat treatments the grain size varied between 300 nm and 5 μm. The combination of SPD and individual heat treatments allows for a systematic study of the ductile to brittle transition (DBT) in the fracture behaviour as a function of grain size. Additionally, the influence of different crack plane orientations was taken into account. The results show that the DBT moves for smaller grain sizes (<1 μm) to higher transition temperatures. Furthermore, large differences in the absolute toughness values for a given temperature for the different crack plane orientations and grain sizes were determined. The findings can be related to a change in the crack path from transcrystalline fracture for grain sizes larger than 1 μm to intercrystalline-dominated fracture for grain sizes smaller than 1 μm.

A. Hohenwarter (✉) · C. Kammerhofer · R. Pippan
Erich Schmid Institute of Materials Science, Austrian Academy of Sciences, Jahnstr. 12, 8700 Leoben, Austria
e-mail: anton.hohenwarter@oeaw.ac.at

C. Kammerhofer
e-mail: christoph.kammerhofer@stud.unileoben.ac.at

R. Pippan
e-mail: pippan@unileoben.ac.at

A. Hohenwarter · C. Kammerhofer · R. Pippan
CD-Laboratory for Local Analysis of Deformation and Fracture, 8700 Leoben, Austria

Introduction

Fatal disasters such as the Titanic's sinking or the Liberty ship incidents during World War II are nowadays known to have their physical origin in the ductile to brittle transition (DBT) of bcc-metals and the associated cleavage fracture in the low temperature regime. The micro-mechanisms of cleavage fracture and the connected transition in the fracture behaviour from brittle to ductile fracture with increasing temperature have extensively been studied and different models have been proposed for the conditions under which cleavage fracture occurs, see, e.g., [1–3]. Contemporaneously, in the last century various severe plastic deformation (SPD) techniques have been developed, which enable to production of ultrafine-grained (UFG) and nanocrystalline (NC) metals by imposing very large strains on coarse-grained starting materials. Due to the strong grain-refinement these materials posses mostly enhanced mechanical and physical properties compared to their coarse-grained counterparts [4–6].

The aforementioned DBT of the fracture behaviour and especially its transition temperature, primarily important in bcc metals with few exceptions, often plays an important role for a safe implementation of materials as can be seen from the examples mentioned earlier. For that reason such studies also have to be performed with UFG and NC metals in case they were considered for structural applications in future. Additionally, SPD in combination with subsequent heat-treatments allows the unique possibility to perform basic studies of the DBT-temperature (DBTT) by varying the grain size and thus the yield stress in a wide range and down to grain sizes, which have not been accessible with classical deformation techniques such as rolling and subsequent annealing up to now. In contrast to other techniques such as electrochemical deposition, the purity of the

material is here solely given by the starting material and no remaining porosity, as to be considered for powder consolidation, has to be taken into account to be major factors influencing the fracture test results.

In this paper, a detailed study into the DBT depending on the grain size ranging from a few hundred nanometers up to classical grain sizes in the micrometer range will be presented. Additionally, the influence of the crack plane orientation on the fracture behaviour was accounted for and discussed.

Experimental

The composition of ARMCO-iron used in this study is 0.009 wt% C, 0.060 wt% Mn, 0.009 wt% P, 0.007 wt% S and the balance Fe. The HPT discs had a diameter of 30 mm and a thickness of 9 mm and were annealed at 800 °C for 1 h prior to HPT deformation. The discs were subjected to 10 revolutions at room temperature at a nominal pressure of 2.8 GPa. Afterwards, Compact-tension (CT) specimens were extracted from the HPT disc with two different crack plane orientations. In Fig. 1, the HPT sample, the extracted specimens and the coordinate system used are displayed with the radial, tangential and axial directions indicated. The difference between the tangential and the radial direction (RD) should be noted. RD is the direction heading into the centre of the disc, whereas the tangential direction (TD) describes the tangential to the circumference of the disc at a particular radius. The specimens' orientation was named after the expected crack propagation direction according to the coordinate system (Fig. 1) resulting in a tangential and a radial specimen orientation.

The geometry of the specimens as well as the calculation of the fracture toughness was based on the recommendations of the ASTM standard E-399. The specimens had a width, W, of 5.2 mm, an initial crack length, a, of $\sim$2.6 mm and a thickness, B, of $\sim$2.6 mm. The fatigue pre-crack was introduced under cyclic compression loading [7].

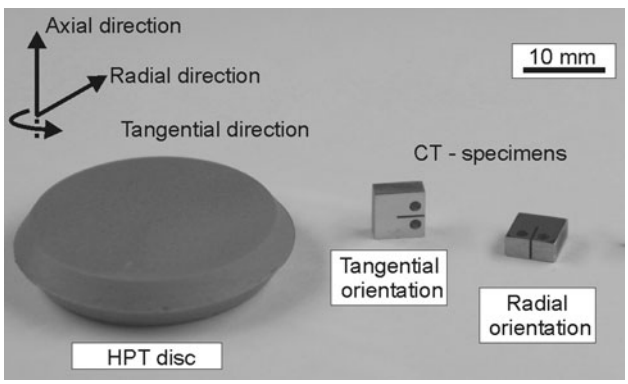

Fig. 1 Photograph presenting the fracture specimens with their different crack orientations machined from the HPT disc

Table 1 Summary of the heat-treatment conditions

Microstructure	Heat-treatment conditions	Hardness HV 0.2
SPD	–	423 ± 2
300 nm	350 °C for 1 h	328 ± 3
1 μm	450 °C for 2 h	212 ± 4
5 μm	650 °C for 1 h	117 ± 4

Along with the SPD-microstructure, different nominal grain sizes, such as 300 nm, 1 and 5 μm were investigated. The grain sizes were adjusted with individual heat-treatments. The heat-treatment conditions for the individual grain sizes and the resulting hardness values can be found in Table 1. All specimens were taken from an area in the former HPT disc, where a saturation in grain-refinement has taken place and therefore a homogenous hardness along the radius was achieved as shown in [8] with hardness measurements after comparable deformation conditions.

The fracture toughness tests were performed on a testing machine from Zwick (Zwick 1382) at a cross-head speed of 400 μm/min. In order to adjust the individual temperatures the specimens were either tested in liquid nitrogen or for the interval between −196 °C and room-temperature in a cooling chamber and for higher temperatures in a heating chamber. The microstructure and the fracture surfaces were characterized with a Zeiss 1525 scanning electron microscope (SEM). Microhardness measurements were performed with a Vickers indenter and a load of 200 gf and 5 indents were averaged.

Results

Microstructure

In Fig. 2a–d, a series of SEM-images of the investigated microstructures, looking into the RD, are presented, see also coordinate system in Fig. 2a, which is the same for all micrographs. In Fig. 2a, the ultrafine-grained structure in the steady state of deformation is shown. In this context, the term steady state is used to describe the fact that a further increase in strain would not lead to an additional refinement of the microstructure, as shown for instance in [9, 10]. Typical for the radial observation direction an elongated grain structure can be observed. Additionally, a certain inclination of the structural elements with respect to

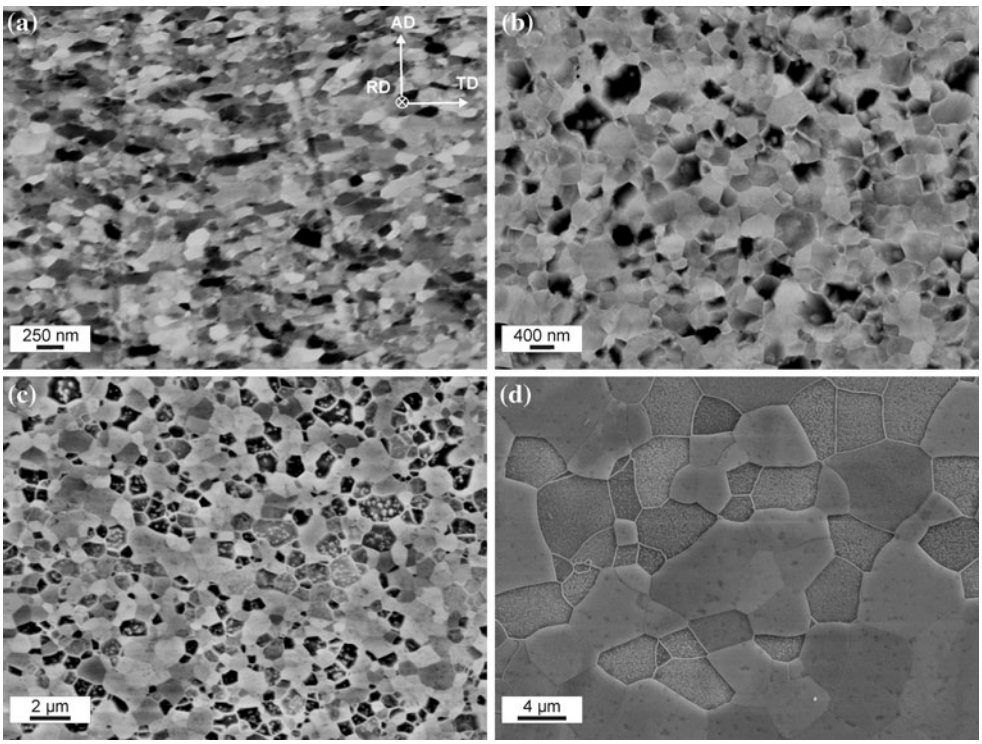

Fig. 2 Typical micrographs of the investigated microstructures looking into the RD of the HPT disc. **a** SPD microstructure showing an elongated microstructure aligned into the shear direction. Heat-treated microstructures with nominal grain-sizes of **b** 300 nm, **c** 1 µm and **d** 5 µm with an equiaxed grain structure

the shear deformation direction, which is parallel to the long margins of Fig. 2a is present, which is simultaneously the TD. These microstructural findings are similar to other reports dealing with ultrafine-grained metals investigated in the same direction [11]. In Fig. 2b–d, the heat-treated microstructures are shown with different nominal grain sizes of 300 nm (Fig. 2b), 1 µm (Fig. 2c) and 5 µm (Fig. 2d). As usual, the heat-treatments, which caused recrystallization, lead to an increase in grain size and thus a decrease in hardness, see Table 1. However, as the micrographs show, also the aspect-ratio of the grain structure is changed. It seems that the elongated SPD microstructure changes to a more equiaxed structure for the 300 nm and larger grain sizes.

Fracture toughness results

General remark

In Figs. 3 and 4, a summary of all fracture tests for the tangential orientation as well as for the radial orientation is presented. Each data point corresponds to a single measurement. Small arrows next to data points are set to indicate that these specimens fractured in a ductile manner and did not meet small scale yielding conditions. For that reason, e.g., specimens with a mean grain size of 5 µm, see

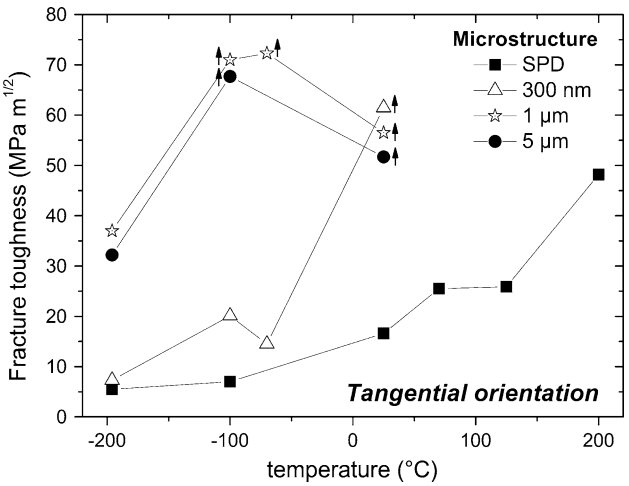

Fig. 3 Summary of the fracture toughness measurements for the tangential orientation. *Arrows* next to data points imply that the values must be regarded as lower bound values for the real fracture toughness

Fig. 3, show after an increase in the fracture toughness from −196 °C to −100 °C, an "apparent" drop in the fracture toughness at room temperature. In such a case the yield strength is already too small with respect to the restricted specimen dimensions so that small scale yielding conditions do not prevail anymore. These data points must

be regarded as a lower bound for the real fracture toughness. In reality, an increase of the fracture toughness compared to valid data points at lower testing temperatures is to be assumed. In such a case no further measurements were performed at higher temperatures. The scatter of the data points with regard to the possible inaccuracy of the measurement of the geometrical parameters of the specimens and the force was evaluated to be smaller than 1 MPam$^{1/2}$ through uncertainty analyses.

Tangential orientation

As Fig. 3 shows, the SPD-microstructure has the lowest fracture toughness values along the entire temperature interval and of all studied microstructures. The fracture toughness is continuously increasing in the investigated temperature range from 5.5 MPam$^{1/2}$ at −196 °C to 48.2 MPam$^{1/2}$ at 200 °C. Regarding the 300-nm specimens, in the lower temperature range (−196 °C to −70 °C) the toughness values are comparable to those of the SPD specimens. However, at ambient temperatures already a large difference compared to the SPD state was determined with an estimated value of 61.5 MPam$^{1/2}$. As explained, the arrow indicates that the value is just a lower estimate of the real fracture toughness. For grain sizes of 1 and 5 µm at −196 °C a value approximately 4 times larger as for the submicrocrystalline states was measured, 37 MPam$^{1/2}$ and 32.2 MPam$^{1/2}$, respectively. For both material states the measurements become invalid at −100 °C. This indicates that the real fracture toughness is even higher and leads to the conclusion that the DBTT is lower for the submicrocrystalline material states, SPD microstructure and 300 nm grain size.

Radial orientation

Specimens with radial specimen orientation show a different picture in Fig. 4. The SPD and the 300 nm specimens have almost the same fracture toughness values at −196 °C and room temperature. However, at −196 °C the values are approximately 4 times larger than in the tangential specimen orientation. In contrast to this, the microcrystalline specimens have again a higher fracture toughness at −196 °C than the submicrocrystalline ones, but are comparable to the measurements of the tangential specimen orientation of the same grain size. At higher testing temperatures the values for the fracture toughness values again increase tremendously. Since the measurements become invalid before room temperature is reached it can be concluded that the DBTT is again lower for the microcrystalline states compared to the submicrocrystalline samples.

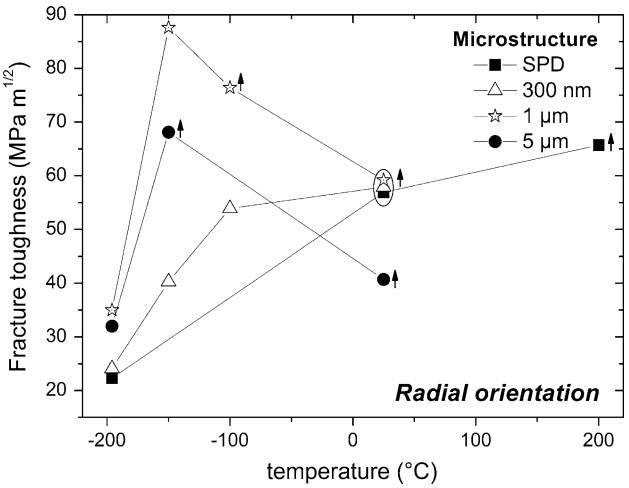

Fig. 4 Summary of the fracture toughness measurements for the radial specimen orientation. *Arrows* next to data points imply that the values must be regarded as lower bound values for the real fracture toughness

Discussion

Dependency of the DBTT on grain size

One of the major results of this experimental study is that the DBTT moves for the smaller grain sizes to higher temperatures, which is at first in contrast to other studies dealing with this topic see for instance [12, 13]. In the following section fractographs will be presented, which are helpful for the discussion of this point.

Fractography of the tangential orientation

In Fig. 5a–c, the typical fracture surfaces of Fe-SPD tested at −196 °C (a), 70 °C (b) and 200 °C (c) are presented. Also displayed is the used coordinate system, showing that in these specimens the crack propagation direction is in the TD and the fracture surface is oriented looking into the axial direction (AD). At −196 °C a granular structure on the fracture surface is visible. Intercrystalline grain boundary fracture occurs, which leads to the rather low measured fracture toughness of about 5.5 MPam$^{1/2}$ at cryogenic temperatures. The same fracture type was also found at room temperature and discussed in [14] more in detail. With increasing temperature grain boundary fracture still occurs, however also more plastification in the shape of steps and ledges, see Fig. 5b, which causes an increase in the fracture toughness, can also be found. Finally, at a testing temperature of 200 °C dimple fracture can be found, Fig. 5c. In Fig. 5c (inset picture), one of the dimples is magnified. Here it can be recognized that the dimple wall surrounds a cluster of grains, which form the nucleation point for void formation and growth.

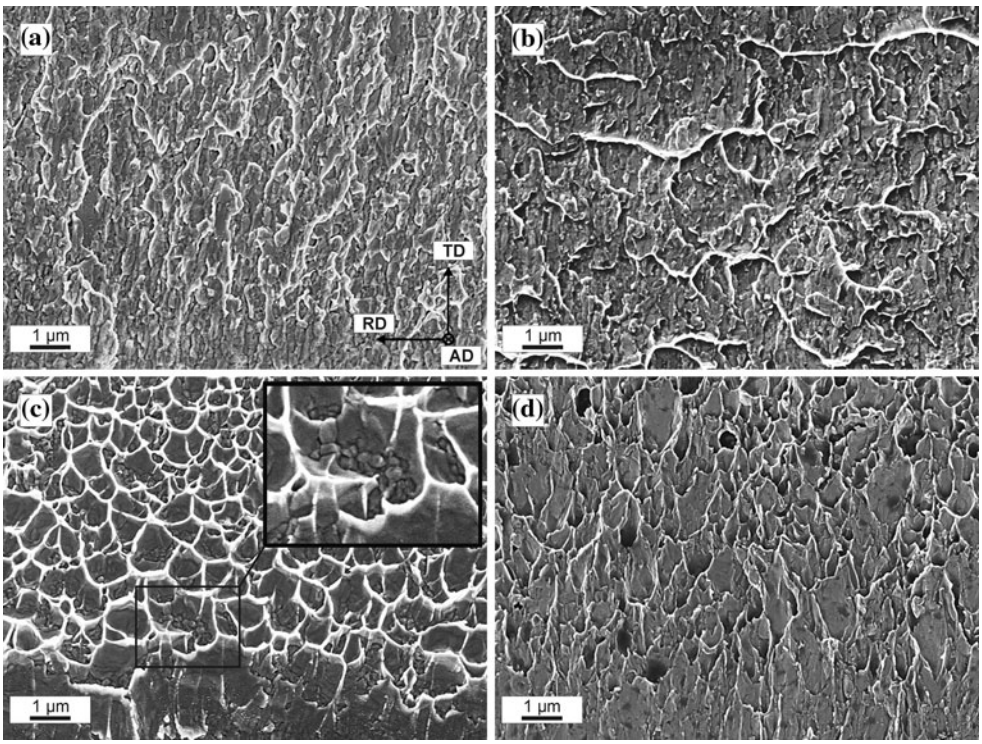

Fig. 5 Representative fractographs demonstrating important features of the different fracture types found in submicrocrystalline specimens with tangential specimen orientation. SPD specimens tested at **a** −196 °C revealing intercrystalline fracture. **b** SPD specimen tested at 70 °C showing evidences of increased plasticity. **c** SPD specimen tested at 200 °C with dimple fracture and **d** a specimen with a nominal grain size of 300 nm already exhibiting dimple fracture at room temperature

In general, it could be assumed that the DBTT decreases with the grain size. This follows directly from the well known Yoffee diagram. For a given grain size the effective yield stress, $\sigma_{y,}$ for the onset of plastic deformation at the crack tip is compared with the brittle fracture stress, σ_b [15]. In this rather simple model, the fracture type depends on the stress level which is reached first behind the crack tip, either the effective yield stress, promoting ductile fracture, or the brittle fracture stress leading to brittle fracture. Whereas σ_y decreases strongly with increasing temperature, σ_b is fairly independent on the temperature, but increases with decreasing grain size. This is due to the fact that a smaller grained microstructure provides a higher density of grain boundaries to stop or even blunt a crack. To conclude, one method to decrease the DBTT is to increase σ_b by decreasing the grain size. These considerations are based on the occurrence of a transcrystalline crack path, where the crack runs on low indicated crystallographic planes. However, in this study intergranular fracture occurred and therefore it seems that the model mentioned before cannot apply.

The intergranular fracture type is often associated with a certain type of grain boundary embrittlement, where sulphur and phosphor are well known examples in connection with steels leading to a pronounced grain boundary embrittlement. In this study an iron with a rather high purity was chosen, see the experimental section, and the heat-treated microstructures show a different behaviour. These factors weaken the impurity argument, as follows.

Regarding the 300-nm samples of the same specimen orientation, it was found that the fracture toughness values are comparable to the SPD values for measurements below room temperature. Also in this temperature regime intercrystalline fracture occurred as shown in Fig. 5a for the SPD specimen. However, at room temperature a large difference in the fracture toughness was found. This is also reflected on the fracture surface by dimple formation, see Fig. 5d. These dimples are elongated since they are part of the stretched zone. After this stretched zone intergranular fracture sets in again (not shown here). The stretched zone could be formed due to a larger deformation capacity of the 300 nm state compared to the SPD state. Specimens with 1 µm grain size having the same specimen orientation, Fig. 6a, show at cryogenic temperature after strong crack blunting, a mixture of intercrystalline and transcrystalline fractured grains. In a more detailed view in Fig. 6b it can be seen that transcrystalline fracture occurs in the larger grains, where a typical feature of transcrystalline fracture, river patterns, can be found. Specimens with 5 µm grain size also exhibit first a stretched zone before exclusively

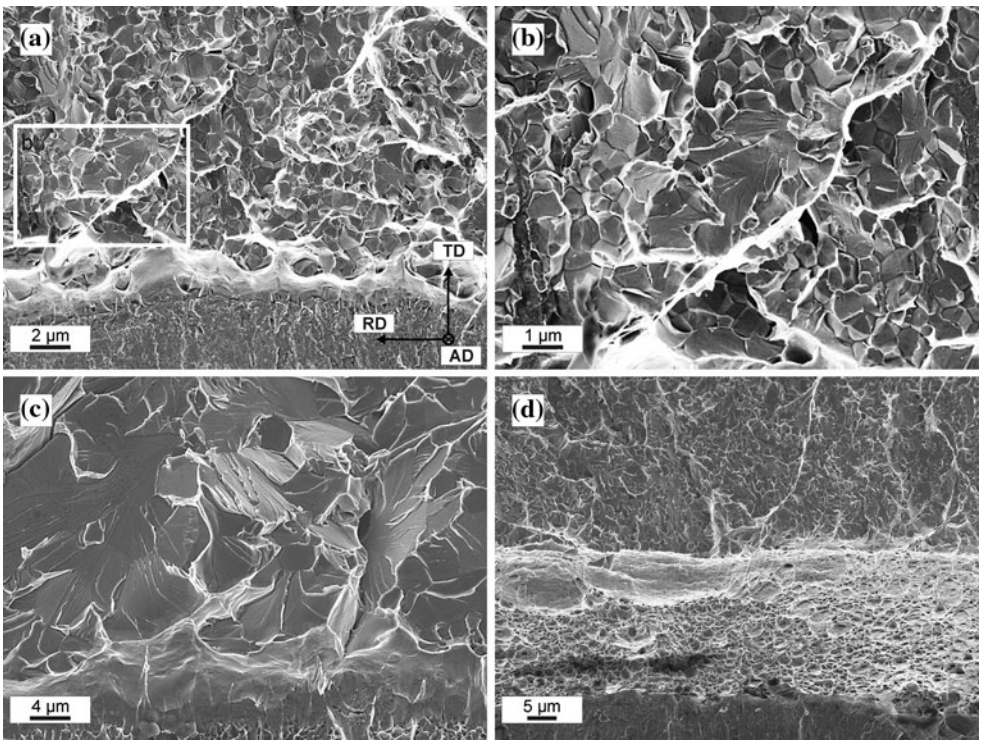

Fig. 6 Fractographs presenting fracture surfaces of specimens with microcrystalline grain size with tangential orientation. **a** Specimen with 1 µm nominal grain size tested at −196 °C. **b** Detail of (**a**) revealing intercrystalline fracture and also areas of transcrystalline fracture. **c** Specimen with 5 µm nominal grain size tested at −196 °C showing fully transcrystalline fracture. **d** Specimen with 1 µm grain size tested at −100 °C with ductile dimple fracture followed by brittle intercrystalline fracture

transcrystalline fracture sets in, Fig. 6c. At a higher testing temperature, for example a specimen with 1 µm grain size tested at −100 °C in Fig. 6d, ductile fracture occurs before in the upper part of the image again intercrystalline fracture can be found. Despite this the fracture toughness determined by means of linear elastic fracture mechanics (LEFM) strongly increases and becomes invalid. Although the fracture type is different for the 1 and 5 µm specimens, the fracture toughness values at −196 °C are more or less the same. Surprisingly, the microcrystalline specimens (1 and 5 µm grain size) show both a crack blunting behaviour before cleavage fracture sets in.

The occurrence of classical ductile fracture for grain sizes starting from 1 µm below room temperature and the large ductile stretched zone of the 300 nm specimen at room temperature gives the hint that intercrystalline fracture of the SPD structure is not due to an impurity embrittlement. When we assume that remaining impurities are dragged along the grain boundaries during the heat-treatments, which is classically the case, the amount of impurities should increase with increasing grain size as the fraction of grain boundaries decreases. Therefore, these microstructures (larger than SPD) are more prone to fail through grain boundary embrittlement at −196 °C. On the contrary even a blunting for the 1 and 5 µm specimens was found. Additionally, at room temperature the microcrystalline specimens showed full ductile fracture and even the 300 nm specimen showed dimple fracture at least within a large stretched zone before brittle fracture set in. In contrast to this the SPD state showed brittle behaviour at room temperature. To conclude, the intercrystalline crack path seems to be an intrinsic property of ultrafine grained Armco-iron that is not caused by impurities, but eventually leads to the lower DBTT for submicrocrystalline iron.

The reason for this property is not yet clear, however, simulations on NC iron [16] indicate that under certain conditions an intercrystalline crack path in NC iron could be observed by the formation of voids in front of the crack tip, which coalesce with the crack tip along the grain boundary.

Also the strong alignment and their aspect ratio could be contributing to the observed crack path and the associated low fracture toughness. In reference [14] a method to increase the fracture toughness was discussed where after deformation via HPT the deformation path is changed and as a result a mixture of elongated and equiaxed grains was obtained. This microstructure showed still intercrystalline fracture, however a larger fracture toughness due to a stronger blunting of the crack tip. To conclude, the small grain size with the connected high hardness, the aspect

ratio of the grains and the alignment of them seem to be factors contributing to the occurence of the intercrystalline crack path.

The influence of the crack plane orientation on the DBTT

The microcrystalline specimens of the radial testing direction show more or less the same mechanical behaviour like those of the tangential orientation, see Fig. 4. Additional fractographic studies revealed the same features as for the first testing direction already presented before. That implies that the microcrystalline specimens, show no influence of the crack plane orientation on the fracture results. However, comparing the results in Figs. 3 and 4 for SPD and 300-nm specimens, both testing directions reveal large differences in the absolute fracture toughness values in the low temperature regime. For example, regarding the SPD state tested at −196 °C the fracture toughness has improved from 5.5 $MPam^{1/2}$ to 22.3 $MPam^{1/2}$, which is by a factor of ∼4. Almost the same increase was found for room temperature experiments for the SPD microstructure. Through fractographic studies this exceptional toughening can be explained.

Fractography of the radial orientation

In Fig. 7a an overview fractograph of the SPD microstructure tested at −196 °C is presented. Additionally, the coordinate system is displayed, and is the same for all three micrographs. In the lower part of the image the fatigue precrack is visible. The overload fracture has single secondary cracks or delaminations which are parallel to the crack propagation direction, which is the RD. Such delaminations are well known to increase the fracture toughness of a material. This delamination induced toughening mechanism is explained for instance by Hertzberg [17]. The stress state in the immediate vicinity in front of the crack tip consists of very high tensile stresses due to the high tensile triaxiality. Through the occurrence of these delaminations the stress component in the thickness direction of the specimen is reduced and the specimen behaves like an array of thin specimens, which usually exhibit a higher fracture toughness. In order to understand the origin of the delaminations better, Fig. 1 must be examined again. Here it can be seen that for specimens with tangential orientation the crack opening direction will be the AD of the HPT sample according to the used coordinate system. The delaminations of specimens with the radial specimen orientation also have the AD as the crack opening direction, see

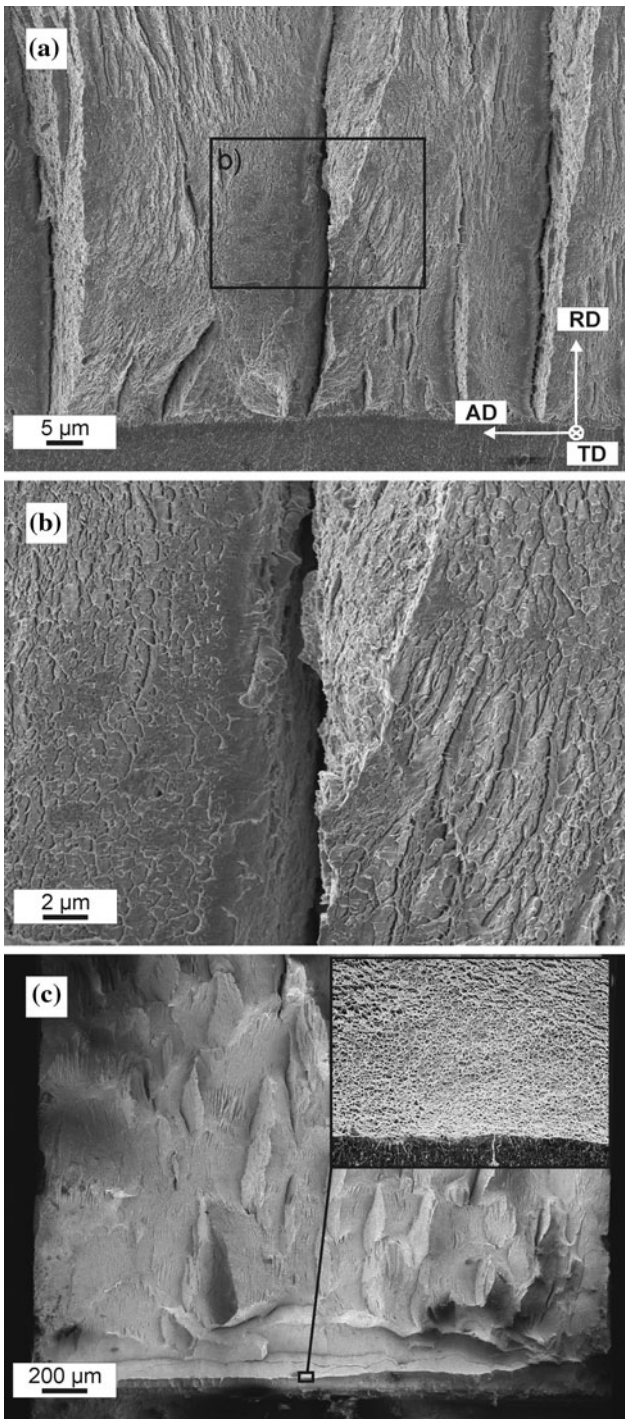

Fig. 7 Selection of fractographs presenting fracture surfaces of specimens with a radial specimen orientation: **a** Overview fractograph of SPD iron tested at −196 °C showing delamination cracks perpendicular to the actual fracture surface. **b** Detailed view of (**a**) revealing a dimpled fracture surface between a delamination. **c** Overview of a specimen with nominal grain size 300 nm tested at room temperature showing dimple fracture (inserted micrograph) followed by various delaminations

Fig. 7a. Therefore, it can be concluded that the occurrence of the delamination is promoted by the low fracture toughness of the tangential orientation, which was previously discussed in "Fractography of the tangential orientation" section, when it can be assumed that pre-existing flaws are present.

These delaminations divide the specimen into smaller ligaments which experience a less pronounced triaxiality. The plane stress state allows plastic deformation, which can be seen in a higher magnification of Fig. 7a better, visible in Fig. 7b. Here many small dimples can be found, which can form between the material delaminations. At this stage it should be pointed out that in this case the improvement of the toughness is here not accomplished by the small grain size but rather by the low fracture toughness of the other testing direction discussed before. Since the mechanical measurements of the specimens with microcrystalline microstructures become invalid before room temperature is reached, compared to the 300 nm specimens, it can be assumed that the fracture toughness is again higher leading to a lower DBTT for the microcrystalline states compared to the submicrocrystalline samples. Although dimples can be found at liquid nitrogen temperature in the SPD and 300 nm states, the fracture toughness is still lower for the submicrocrystalline specimens compared to their microcrystalline counterparts which show transcrystalline fracture already.

At room temperature the delamination-induced toughening mechanism is still working for the SPD state and partly also for the specimen with 300 nm grain size, which is illustrated in Fig. 7c, where still many delamination can be seen on the fracture surface. However, at the very beginning of the overload fracture surface also a large stretched zone is visible consisting of fine dimples, see detailed image section in Fig. 7c. This stretched zone indicates the high fracture toughness. For larger grain sizes delaminations cannot be found and therefore the fracture behaviour becomes more or less isotropic.

Conclusions and summary

In this paper the fracture behaviour of a bcc metal, ARMCO-iron, as a function of the grain size in a wide range of testing temperatures was analyzed. The main results are as follows:

1. It was found that the DBTT is higher for submicrocrystalline grain sizes compared to microcrystalline microstructures. This behaviour was related to the intercrystalline crack path for grain sizes smaller than 1 μm.
2. Simultaneously this crack path and the connected low fracture toughness favours the anisotropy of the fracture behaviour. Due to delamination induced toughening a pronounced increase in the fracture toughness for the radial specimen orientation was achieved.
3. Interesting for room temperature applications it could be shown that a heat-treatment increasing the grain size from the SPD state (200 nm) to 300 nm can increase the fracture toughness significantly.

In the future the analyses of the plastic deformation behaviour by tensile or compression tests ranging from −196 °C to room temperature should help for a deeper understanding of the observed fracture mechanism, especially for the understanding of the intercrystalline crack path.

Acknowledgement The work was partly supported by the Austrian Science Fund FWF in the framework of Research Network S 10402 N16.

References

1. Griffith AA (1920) Philos Trans R Soc Lond 221:163
2. Rice JR, Thomson R (1974) Phil Mag 29:73
3. Chen JH, Wang Q, Wang GZ, Li Z (2003) Acta Mater 51:1841
4. Meyers MA, Mishra A, Benson DJ (2006) Prog Mater Sci 51:427
5. Valiev RZ, Islamgaliev RK, Alexandrov IV (2000) Prog Mater Sci 45:103
6. Zhilyaev AP, Langdon TG (2008) Prog Mater Sci 53:893
7. Suresh S (1985) Eng Frac Mech 21:453
8. Hohenwarter A, Bachmaier A, Gludovatz B, Scheriau S, Pippan R (2009) Int J Mater Res (formerly Z.Metallkunde) 100:1653
9. Vorhauer A, Pippan R (2004) Scripta Mater 51:921
10. Xu C, Horita Z, Langdon TG (2008) Acta Mater 56:5168
11. Vorhauer A, Pippan R (2008) Metall Mater Trans A 39:417
12. Song R, Ponge D, Raabe D (2005) Acta Mater 53:4881
13. Inoue T, Yin F, Kimura Y, Tsuzaki K, Ochiai S (2009) Metall Mater Trans A 41:341
14. Hohenwarter A, Pippan R (2010) Mater Sci Eng A 527:2649
15. Morries JW (2008) Science 320:1022
16. Latapie A, Farkas D (2004) Phys Rev 69:134110-1
17. Hertzberg RW (1996) Deformation and fracture mechanics of engineering materials. Wiley, New York